Stationary Transversal Hot Zones in Adiabatic Packed-Bed Reactors

G. Viswanathan and D. Luss
Dept. of Chemical Engineering, University of Houston, Houston, TX 77204

A. Bindal and J. Khinast
Dept. of Chemical and Biochemical Engineering, Rutgers University, Piscataway, NJ 08854

DOI 10.1002/aic.10542
Published online August 3, 2005 in Wiley InterScience (www.interscience.wiley.com).

A pseudo-homogeneous model predicts that a stationary, stable, transversal nonuniform temperature pattern cannot form in any cross section of an adiabatic packed-bed reactor used to conduct a single reaction, if its dynamics depends only on the concentration of a limiting reactant and temperature. This is due to the fact that the transversal heat dispersion in the reactor is larger than that of the limiting reactant. This conclusion is proved for a shallow packed-bed reactor described by a pseudo-homogeneous model. Extensive numerical simulations showed that a two-phase model of an adiabatic packed-bed reactor exhibits the same behavioral features. A stable, stationary hot zone can form in the cross section of the reactor only under the unrealistic assumption that the transversal species dispersion exceeded that of the temperature. © 2005 American Institute of Chemical Engineers *AIChE J,* 51: 3028–3038, 2005
Keywords: packed-bed reactor, hot spot, neutral stability, temperature pattern, nonuniform perturbations

Introduction

Localized hot zones have been reported to exist in packed-bed reactors. They have in general a deleterious impact on the performance of the reactor, that is, decreasing the yield of the desired products. Moreover, they may initiate undesired results, leading to runaway reactions. Puszynski and Hlavacek[1] observed a periodic generation of a downstream traveling hot region during CO oxidation in a packed-bed reactor. Wicke and Onken[2,3] observed a similar periodic, traveling temperature wave during the oxidation of either CO or ethylene in a packed-bed reactor. They pointed out that these periodic temperature waves form, when the catalytic reaction rate in the upstream section of the reactor is oscillatory. Rovinski and Menzinger[4] observed a periodic sequence of traveling concentration pulses when they conducted a Belousov–Zhabotinski reaction in a catalytic packed-bed reactor under excitable conditions. Sheintuch research group[5-7] conducted extensive theoretical analyses of the formation of these traveling hot zones.

A uniform temperature is expected to exist at any cross section of adiabatic packed-bed reactors. There have been several attempts to predict the conditions that may lead to evolution of a stable, nonuniform transversal temperature field in such a reactor. Matros[8] reported formation of hot zones in a packed-bed reactor in which the catalyst was not uniformly packed. This type of hot zone formation may be circumvented by improving the packing of the bed and will not be addressed here. Barkelew and Gambhir[9] reported the formation of small clumps of molten catalyst (clinkers) during hydrodesulfurization in trickle-bed reactors. Wicke and Onken[2,3] noted that the temperature at two locations in the same cross section of the reactor was different, that is, transversal (normal to the flow direction) temperature patterns existed. When local hot regions exist next to the reactor walls, they may decrease its strength, leading to severe safety problems. A thorough understanding and ability to predict when such local hot zones form are

Correspondence concerning this article should be addressed to D. Luss at dluss@uh.edu.

paramount for a rational reactor design and operation that circumvent this undesired behavior.

Several studies attempted to predict the conditions leading to formation of the transversal hot zones. Viljoen et al.[10] pointed out that an exothermic chemical reaction may generate various convection and temperature patterns in a porous media. Stroh and Balakotaiah,[11] Nguyen and Balakotaiah,[12,13] and Subramanian and Balakotaiah[14] all showed that spatiotemporal flow and temperature patterns may evolve in packed-bed reactors, when the feed flow rate is rather low. Schmitz and Tsotsis[15] found that stationary patterns can form in a chain of interacting catalysts (cell model) only when the rate of species exchange exceeded that of heat exchange. Balakotaiah et al.[16] showed that the uniform stable state in an adiabatic packed-bed reactor may become unstable, leading to evolution of a nonuniform state. They showed that the larger the diameter of the reactor, the larger the number of possible stationary nonuniform states that may form. Yakhnin and Menzinger[17] pointed out that the analysis of Balakotaiah et al.[16] was for a case in which the transversal effective heat dispersion was lower than that of the species dispersion. This condition is similar to that enabling formation of stationary patterns in two variable reaction–diffusion systems, if the diffusion of the inhibitor is larger than that of the activator.[18,19] However, in practice the transversal dispersion of heat in a packed-bed reactor is always larger than that of the species dispersion.

The goal of this study is to determine under what conditions and reaction rates stable, stationary, nonuniform temperature states exist in packed-bed reactors, and to analyze the qualitative features and stability characteristics of the branches of the nonuniform states.

Mathematical Model

We use a heterogeneous or two-phase model to describe an adiabatic packed-bed reactor. The corresponding energy and limiting species balances for both the gas and the solid phases are as follows

$$(\rho C_p)_f \varepsilon \frac{\partial T_f}{\partial t} = -(\rho C_p)_f v \frac{\partial T_f}{\partial z} + \varepsilon \lambda_{f,a} \frac{\partial^2 T_f}{\partial z^2} + \varepsilon \lambda_{f,\perp} \nabla_\perp^2 T_f + h a_v (T_s - T_f) \quad (1)$$

$$\varepsilon \frac{\partial C_f}{\partial t} = -v \frac{\partial C_f}{\partial z} + \varepsilon D_{f,a} \frac{\partial^2 C_f}{\partial z^2} + \varepsilon D_{f,\perp} \nabla_\perp^2 C_f - k a_v (C_f - C_s) \quad (2)$$

$$(\rho C_p)_s (1 - \varepsilon) \frac{\partial T_s}{\partial t} = (1 - \varepsilon) \lambda_{s,\perp} \nabla_\perp^2 T_s + (1 - \varepsilon) \lambda_{s,a} \frac{\partial^2 T_s}{\partial z^2} - h a_v (T_s - T_f) + (-\Delta H) \bar{r}(C_s, T_s) \quad (3)$$

$$\frac{dC_s}{dt} = -k a_v (C_f - C_s) + \bar{r}(C_s, T_s) \quad (4)$$

where T_f and T_s are the fluid- and solid-phase temperatures, C_f and C_s are the fluid- and solid-phase concentrations, v is the superficial gas velocity, $\bar{r}(C_s, T_s)$ is the reaction rate, and

$$\nabla_\perp^2 = \left[\frac{1}{r} \frac{\partial}{\partial r} \left(r \frac{\partial}{\partial r} \right) + \frac{1}{r^2} \frac{\partial^2}{\partial \phi^2} \right] \quad (5)$$

The corresponding boundary conditions are

$$\left. \begin{aligned} -\varepsilon D_{f,a} \frac{\partial C_f}{\partial z} &= v(C_{in} - C_f) \\ -\varepsilon \lambda_{f,a} \frac{\partial T_f}{\partial z} &= v(\rho C_p)_f (T_{in} - T_f) \\ \frac{\partial T_s}{\partial z} &= 0 \end{aligned} \right\} \quad z = 0 \quad (6)$$

$$\frac{\partial C_f}{\partial z} = 0 \qquad \frac{\partial T_f}{\partial z} = 0 \qquad \frac{\partial T_s}{\partial z} = 0 \qquad z = L \quad (7)$$

$$\frac{\partial C_f}{\partial r} = 0 \qquad \frac{\partial T_f}{\partial r} = 0 \qquad \frac{\partial T_s}{\partial r} = 0 \qquad r = R \quad (8)$$

Because the characteristic reaction time is very small relative to the others in the system the solid reactant concentration may be described by a pseudo-steady-state equation (that is, ignoring the time derivative in Eq. 4). For certain kinetics this enables one to obtain an explicit solution for C_s that can be substituted into the rate expression. For example, for a first-order reaction

$$C_s = \frac{C_f}{1 + \left(\frac{k_\infty}{k a_v} \right) \exp\left(\frac{-E}{\bar{R} T_s} \right)} \quad (9)$$

This substitution reduces the model to three equations for T_f, C_f, and T_s. By introducing the following dimensionless variables

$$\theta = (T - T_{in})/T_{in} \qquad x = (C_{in} - C)/C_{in}$$

$$\gamma = \frac{E}{\bar{R} T_{in}} \qquad \beta = \frac{(-\Delta H) C_{in}}{(\rho C_p)_f T_{in}}$$

$$\mathrm{St}_m = vL/(k a_v) \qquad \mathrm{St}_h = vL/(h a_v)$$

$$\mathrm{Pe}_{f,a}^h = \frac{vL}{\varepsilon \lambda_{f,a}/(\rho C_p)_f} \qquad \mathrm{Pe}_{f,a}^m = vL/\varepsilon D_{f,a}$$

$$\mathrm{Pe}_{s,a}^h = \frac{vL}{(1 - \varepsilon) \lambda_{s,a}/(\rho C_p)_f} \qquad \mathrm{Pe}_{f,\perp}^h = \frac{vR^2}{L \varepsilon \lambda_{f,\perp}/(\rho C_p)_f}$$

$$\mathrm{Pe}_{f,\perp}^m = vR^2/(L D_{f,\perp \varepsilon}) \qquad \mathrm{Pe}_{s,\perp}^h = \frac{vR^2}{L \varepsilon \lambda_{s,\perp}/(\rho C_p)_f}$$

$$\mathrm{Le} = \varepsilon + (1 - \varepsilon) \frac{(\rho C_p)_s}{(\rho C_p)_f} \quad (10)$$

the model becomes

$$\frac{\partial \theta_f}{\partial \tau} = \frac{1}{\varepsilon} \left[\frac{1}{\mathrm{Pe}_{f,\perp}^h} \nabla_\perp^2 \theta_f + \frac{1}{\mathrm{Pe}_{f,a}^h} \frac{\partial^2 \theta_f}{\partial \eta^2} - \frac{\partial \theta_f}{\partial \eta} + \mathrm{St}_h (\theta_s - \theta_f) \right] \quad (11)$$

$$\frac{\partial x_f}{\partial \tau} = \frac{1}{\varepsilon}\left[\frac{1}{\mathrm{Pe}^m_{f,\perp}}\nabla^2_\perp x_f + \frac{1}{\mathrm{Pe}^m_{f,a}}\frac{\partial^2 x_f}{\partial \eta^2} - \frac{\partial x_f}{\partial \eta} + \mathbb{R}(\theta_s, x_f)\right] \quad (12)$$

$$\frac{\partial \theta_s}{\partial \tau} = \frac{1}{(\mathrm{Le} - \varepsilon)}\left[\frac{1}{\mathrm{Pe}^h_{s,\perp}}\nabla^2_\perp \theta_s + \frac{1}{\mathrm{Pe}^h_{s,a}}\frac{\partial^2 \theta_s}{\partial \eta^2} - \mathrm{St}_h(\theta_s - \theta_f) + \beta\mathbb{R}(\theta_s, x_f)\right] \quad (13)$$

where, for a first-order reaction,

$$\mathbb{R}(\theta_s, x_f) = \mathrm{Da}\left[\frac{\exp\left(\frac{\gamma\theta_s}{\theta_s + 1}\right)}{1 + \frac{\mathrm{Da}}{\mathrm{St}_m}\exp\left(\frac{\gamma\theta_s}{\theta_s + 1}\right)}\right](1 - x_f)$$

$$\mathrm{Da} = \frac{Lk_\infty e^{-\gamma}}{v} \quad (14)$$

The corresponding boundary conditions are

$$\frac{1}{\mathrm{Pe}^h_{f,a}}\frac{\partial \theta_f}{\partial \eta} = \theta_f \qquad \frac{1}{\mathrm{Pe}^m_{f,a}}\frac{\partial x_f}{\partial \eta} = x_f \qquad \frac{\partial \theta_s}{\partial \eta} = 0 \qquad \eta = 0 \quad (15)$$

$$\frac{\partial \theta_f}{\partial \eta} = 0 \qquad \frac{\partial x_f}{\partial \eta} = 0 \qquad \frac{\partial \theta_s}{\partial \eta} = 0 \qquad \eta = 1 \quad (16)$$

$$\frac{\partial \theta_f}{\partial \xi} = 0 \qquad \frac{\partial x_f}{\partial \xi} = 0 \qquad \frac{\partial \theta_s}{\partial \xi} = 0 \qquad \xi = 1 \quad (17)$$

When the transport resistances between the solid and fluid phase are small, the reactor may be described by the simpler pseudo-homogeneous ($\mathbb{PH}$) model

$$\frac{\partial \theta}{\partial \tau} = \frac{1}{\mathrm{Le}_{\mathbb{PH}}}\left[\frac{1}{\mathrm{Pe}^h_{\mathbb{PH},\perp}}\nabla^2_\perp \theta + \frac{1}{\mathrm{Pe}^h_{\mathbb{PH},a}}\frac{\partial^2 \theta}{\partial \eta^2} - \frac{\partial \theta}{\partial \eta} + \beta\mathbb{R}(\theta, x)\right] \quad (18)$$

$$\frac{\partial x}{\partial \tau} = \left[\frac{1}{\mathrm{Pe}^m_{\mathbb{PH},\perp}}\nabla^2_\perp x + \frac{1}{\mathrm{Pe}^m_{\mathbb{PH},a}}\frac{\partial^2 x}{\partial \eta^2} - \frac{\partial x}{\partial \eta} + \mathbb{R}(\theta, x)\right] \quad (19)$$

subject to boundary conditions

$$\frac{1}{\mathrm{Pe}^h_{\mathbb{PH},a}}\frac{\partial \theta}{\partial \eta} = \theta \quad \frac{1}{\mathrm{Pe}^m_{\mathbb{PH},a}}\frac{\partial x}{\partial \eta} = x \quad \eta = 0 \quad (20)$$

$$\frac{\partial \theta}{\partial \eta} = 0 \qquad \frac{\partial x}{\partial \eta} = 0 \qquad \eta = 1 \quad (21)$$

$$\frac{\partial \theta}{\partial \xi} = 0 \qquad \frac{\partial x}{\partial \xi} = 0 \qquad \xi = 1 \quad (22)$$

where, for a first-order irreversible reaction,

$$\mathbb{R}(\theta, x) = \mathrm{Da}\exp\left(\frac{\gamma\theta}{\theta + 1}\right)(1 - x) \quad (23)$$

The dimensionless quantities in the pseudo-homogeneous model are

$$\mathrm{Le}_{\mathbb{PH}} = [(\rho C_p)_{\mathbb{PH}}/(\rho C_p)_f] \qquad \mathrm{Pe}^h_{\mathbb{PH},a} = \frac{vL}{\lambda_{\mathbb{PH},a}/(\rho C_p)_f}$$

$$\mathrm{Pe}^m_{\mathbb{PH},a} = \frac{vL}{D_{\mathbb{PH},a}}$$

$$\mathrm{Pe}^h_{\mathbb{PH},\perp} = \frac{vR^2}{L\lambda_{\mathbb{PH},\perp}/(\rho C_p)_f} \qquad \mathrm{Pe}^m_{\mathbb{PH},\perp} = \frac{vR^2}{LD_{\mathbb{PH},\perp}} \quad (24)$$

Vortmeyer and Schaeffer[20] derived a relation for the effective thermal conductivity in this model. Recent studies by Dommeti et al.[15] and Balakotaiah and Dommeti[21] indicate that this relation is not always valid.

Steady-state numerical solutions were obtained by discretizing the spatial derivatives by finite differences in all three directions (102 grid points in the axial direction and 60–100 grid points in the radial and azimuthal directions). In some cases, global orthogonal collocation was used to discretize the radial and azimuthal directions (10–25 points in each direction). The steady-state solutions were computed either by a sparse inexact Newton–Krylov subspace method using ILU preconditioned BiCGSTAB[22] or by a Newton–Raphson iteration procedure using a nonlinear equation solver (NLEQ), direct (LAPACK), and sparse (MA28) solver.[23] The bifurcation diagrams were computed using pseudo-arc length continuation.[24] The branches of the 2-D and 3-D states and of the codimension-1 were calculated using the Library of Continuation Algorithms (LOCA) software.[25,26]

Dynamic simulations were conducted using the Linear Implicit Extrapolator (LIMEX).[27,28] The 1-D calculations were computed using the LAPACK option. The 2-D and 3-D calculations were performed using either the direct linear solver (MA28) or the sparse iterative linear solver (GMRES/BiCGSTAB). The sparse iterative solver in the linear step usually converged in two to three iterations.

Both the steady-state and dynamic simulations of the full model are rather demanding. Thus, we first studied a simplified version of the full model, that of a *shallow reactor*, to gain insight into the structure of the bifurcation diagrams of the states with the nonuniform transversal temperature, and their stability features and transitions. A similar approach was used by Balakotaiah et al.[29] in their study of pattern formation in a shallow monolith reactor. This shallow reactor model was obtained by a Liapunov–Schmidt reduction[30] of the full model. Details of the reduction procedure used in this case are reported by Viswanathan.[31] We denote by θ_f, x_f, and θ_s the spatially averaged quantities in the shallow reactor model, that is

$$\theta_f = \int_0^1 \theta_f d\eta \qquad x_f = \int_0^1 x_f d\eta \qquad \theta_s = \int_0^1 \theta_s d\eta \quad (25)$$

The shallow-reactor two-phase model is

$$\frac{d\theta_f}{d\tau} - \frac{1}{\varepsilon}\left[\frac{1}{\mathrm{Pe}^h_{f,\perp}}\nabla^2_\perp\theta_f - \theta_f + \mathrm{St}_h(\theta_s - \theta_f)\right] = 0 \qquad (26)$$

$$\frac{dx_f}{d\tau} - \frac{1}{\varepsilon}\left[\frac{1}{\mathrm{Pe}^m_{f,\perp}}\nabla^2_\perp x_f - x_f + \mathbb{R}(\theta_s, x_f)\right] = 0 \qquad (27)$$

$$\frac{d\theta_s}{d\tau} - \frac{1}{(\mathrm{Le} - \varepsilon)}\left[\frac{1}{\mathrm{Pe}^h_{s,\perp}}\nabla^2_\perp\theta_s - \mathrm{St}_h(\theta_s - \theta_f) + \beta\mathbb{R}(\theta_s, x_f)\right] = 0 \qquad (28)$$

with $\mathbb{R}(\theta_s, x_f)$ defined by Eq. 14. The corresponding boundary conditions are

$$\frac{\partial\theta_f}{\partial\xi} = 0 \qquad \frac{\partial x_f}{\partial\xi} = 0 \qquad \frac{\partial\theta_s}{\partial\xi} = 0 \qquad \xi = 1 \qquad (29)$$

The pseudo-homogeneous model can be reduced in a similar way.

The reduced model was discretized using a second-order central difference scheme. To circumvent the singularity at the center, the grid points were placed at the radial positions $\xi_j = (2j - 1)/(2N - 1)\ \forall\ j = 1, N$.[32] After discretization, the reduced model is similar to a cell model in a circular cross section, with the diffusion terms (in the continuous model) mimicked by exchange coefficients among the cells.

Stationary nonuniform temperature in a shallow reactor

We consider here the evolution and dynamics of stationary temperature patterns in an adiabatic shallow packed-bed reactor ($\mathbb{SR}$) using a pseudo-homogeneous model. This limiting model provides important insight about the dynamic features of the more complex models, the analysis and simulations of which are much more demanding. The mathematical model of this two variables system is

$$\frac{d\theta}{d\tau} - \frac{1}{\mathrm{Le}_{\mathbb{PH}}}\left[\frac{1}{\mathrm{Pe}^h_{\mathbb{PH},\perp}}\nabla^2_\perp\theta - \theta + \beta\mathbb{R}(\theta, x)\right] = 0 \qquad (30)$$

$$\frac{dx}{d\tau} - \left[\frac{1}{\mathrm{Pe}^m_{\mathbb{PH},\perp}}\nabla^2_\perp x - x + \mathbb{R}(\theta, x)\right] = 0 \qquad (31)$$

with $\mathbb{R}(\theta, x)$ defined by Eq. 23. The corresponding boundary conditions are

Table 1. First Nine Eigenvalues Satisfying Eq. 36

No.	m	n	μ_{mn}
1	1	1	1.8412
2	2	1	3.0542
3	0	1	3.8317
4	3	1	4.2012
5	4	1	5.3176
6	1	2	5.3314
7	5	1	6.4156
8	2	2	6.7061
9	0	2	7.0155

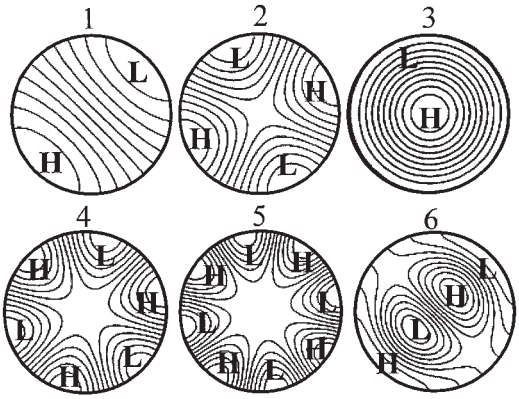

Figure 1. The first six transversal eigenmodes.

$$\frac{\partial\theta}{\partial\xi} = 0 \qquad \frac{\partial x}{\partial\xi} = 0 \qquad \xi_j = 1 \qquad (32)$$

Linear stability analysis predicts that a uniform steady state is stable with respect to uniform perturbations, if the two eigenvalues of

$$\mathbb{L}_1 = \begin{bmatrix} \dfrac{-1}{\mathrm{Le}_{\mathbb{PH}}} + \dfrac{\beta}{\mathrm{Le}_{\mathbb{PH}}}\dfrac{\partial\mathbb{R}}{\partial\theta}\Big|_{(\theta,x)_{ss}} & \dfrac{\beta}{\mathrm{Le}_{\mathbb{PH}}}\dfrac{\partial\mathbb{R}}{\partial x}\Big|_{(\theta,x)_{ss}} \\ \dfrac{\partial\mathbb{R}}{\partial\theta}\Big|_{(\theta,x)_{ss}} & -1 + \dfrac{\partial\mathbb{R}}{\partial x}\Big|_{(\theta,x)_{ss}} \end{bmatrix} \qquad (33)$$

have a negative real part. In a packed-bed reactor, $\mathrm{Le} \gg 1$ and it can be proven that the stability condition

$$\det(\mathbb{L}_1) > 0 \qquad (34)$$

implies that in this system $\mathrm{tr}(\mathbb{L}_1) < 0$. Thus, condition 34 is necessary and sufficient for stability and no Hopf bifurcation can occur from a state satisfying Eq. 34. Next we consider a small nonuniform spatial perturbation of the form

$$\underline{\omega}_{mn}(\xi, \phi) = \begin{bmatrix} \omega_1 J_m(\mu_{mn}\xi)e^{im\phi} \\ \omega_2 J_m(\mu_{mn}\xi)e^{im\phi} \end{bmatrix} \qquad (35)$$

where m and n are the azimuthal and radial mode numbers and $e^{im\phi}$ and $J_m(\mu_{mn}\xi)$ are the corresponding eigenfunctions. Because of the no-flux boundary condition, μ_{mn} satisfies the relation

$$\left.\frac{dJ_m(\mu_{mn}\xi)}{d\xi}\right|_{\xi=1} = mJ_m(\mu_{mn}) - \mu_{mn}J_{m+1}(\mu_{mn}) = 0 \qquad (36)$$

The first nine eigenvalues μ_{mn} of the spatial perturbations are reported in Table 1. Although all the perturbations with $m = 0$ have no azimuthal dependency, all the others depend on both ξ and ϕ. Figure 1 describes the first six eigenmodes. Linear stability analysis of a uniform solution of the steady state of the pseudo-homogeneous model following a small perturbation of $\underline{\omega}_{mn}$, defined by Eq. 35, shows that it is stable to the inhomogeneous perturbations, if both eigenvalues of

$$\mathbb{L}_{\mathbb{PH}}^{\mathbb{SR}} = (\mathbb{L}_1 - \mu_{mn}^2 \mathbb{P}_1) \tag{37}$$

have a negative real part, where

$$\mathbb{P}_1 = \begin{bmatrix} \dfrac{1}{\mathrm{Le}_{\mathbb{PH}} \mathrm{Pe}^h_{\mathbb{PH},\perp}} & 0 \\ 0 & \dfrac{1}{\mathrm{Pe}^m_{\mathbb{PH},\perp}} \end{bmatrix} \tag{38}$$

The neutral stability curve, at which a transition from a uniform to a nonuniform state occurs, is obtained by a simultaneous solution of the uniform steady-state solutions of Eqs. 30–32 and

$$\det(\mathbb{L}_{\mathbb{PH}}^{\mathbb{SR}}) = 0 \tag{39}$$

Condition 39 requires that

$$\mathcal{M}_{\mathbb{PH}} = \frac{\dfrac{\mu_{mn}^2}{\mathrm{Pe}^h_{\mathbb{PH},\perp}} \left[\left(\beta \left. \dfrac{\partial \mathbb{R}}{\partial \theta} \right|_{(\theta,x)_{ss}} - 1 \right) - \dfrac{\mu_{mn}^2}{\mathrm{Pe}^h_{\mathbb{PH},\perp}} \right]}{\left[\mathrm{Le}_{\mathbb{PH}} \{\det(\mathbb{L}_1)\} + \dfrac{\mu_{mn}^2}{\mathrm{Pe}^h_{\mathbb{PH},\perp}} \left(1 - \left. \dfrac{\partial \mathbb{R}}{\partial x} \right|_{(\theta,x)_{ss}} \right) \right]} \tag{40}$$

where

$$\mathcal{M}_{\mathbb{PH}} = \frac{\mathrm{Pe}^m_{\mathbb{PH},\perp}}{\mathrm{Pe}^h_{\mathbb{PH},\perp}} = \frac{\lambda_{\mathbb{PH},\perp}}{D_{\mathbb{PH},\perp}(\rho C_p)_{\mathbb{PH}}} \tag{41}$$

The above condition may be rewritten as

$$\left(1 + \frac{\mu_{mn}^2}{\mathrm{Pe}^h_{\mathbb{PH},\perp}} \right) \mathrm{Le}_{\mathbb{PH}} \{\det(\mathbb{L}_1)\} + \frac{\mu_{mn}^2}{\mathrm{Pe}^h_{\mathbb{PH},\perp}} + \left(\frac{\mu_{mn}^2}{\mathrm{Pe}^h_{\mathbb{PH},\perp}} \right)^2 = (1 - \mathcal{M}_{\mathbb{PH}}) \left[\left(1 + \frac{\mu_{mn}^2}{\mathrm{Pe}^h_{\mathbb{PH},\perp}} \right) \mathrm{Le}_{\mathbb{PH}} \{\det(\mathbb{L}_1)\} + \frac{\mu_{mn}^2}{\mathrm{Pe}^h_{\mathbb{PH},\perp}} \beta \left. \frac{\partial \mathbb{R}}{\partial \theta} \right|_{(\theta,x)_{ss}} \right] \tag{42}$$

The effective heat diffusion in a pseudo-homogeneous model of a packed-bed reactor is always larger than that of the species dispersion, that is, $\mathcal{M}_{\mathbb{PH}} \geq 1$. The lefthand side of Eq. 42 is positive when $\det(\mathbb{L}_1) > 0$. Thus, the condition for a transition from a uniform to a nonuniform state of $\det(\mathbb{L}_{\mathbb{PH}}^{\mathbb{SR}}) = 0$ is not satisfied if $\mathcal{M}_{\mathbb{PH}} \geq 1$. This leads to the important conclusion that for reactions described by the above model *a bifurcation to a stationary nonuniform state from a uniform state, stable to uniform perturbations, cannot occur for the realistic cases of* $\mathcal{M}_{\mathbb{PH}} \geq 1$. However, when $\mathcal{M}_{\mathbb{PH}} \geq 1$, an unstable bifurcation to a nonuniform state may occur from the unstable branch of uniform states for which $\det(\mathbb{L}_1) < 0$. Extensive numerical calculations showed that all the solutions on a branch of nonuniform states are unstable whenever the branch emanates and terminates on the branch of unstable uniform states. Thus, *stable nonuniform states do not exist for the realistic case of* $\mathcal{M}_{\mathbb{PH}} \geq 1$. A stable bifurcation to a nonuniform state may occur from the stable branch only for $\mathcal{M}_{\mathbb{PH}} < 1$.

The two-phase shallow reactor model ($\mathbb{SR}$) consists of three state variables. Its stability analysis is similar, but more intricate. Assuming a small spatial perturbation of the form

$$\begin{bmatrix} \omega_1 J_m(\mu_{mn}\xi) e^{im\phi} \\ \omega_2 J_m(\mu_{mn}\xi) e^{im\phi} \\ \omega_3 J_m(\mu_{mn}\xi) e^{im\phi} \end{bmatrix} \tag{43}$$

the uniform steady-state solution is stable with respect to this perturbation if all eigenvalues of

$$\mathbb{L}_{\mathbb{TP}}^{\mathbb{SR}} = (\mathbb{L}_2 - \mu_{mn}^2 \mathbb{P}_2) \tag{44}$$

have a negative real part, where (the subscript $\mathbb{TP}$ denotes two-phase)

$$\mathbb{L}_2 = \begin{bmatrix} \dfrac{1}{\varepsilon}(-1 - \mathrm{St}_h) & 0 & \dfrac{\mathrm{St}_h}{\varepsilon} \\ 0 & \dfrac{1}{\varepsilon}\left(-1 + \left. \dfrac{\partial \mathbb{R}}{\partial x_f} \right|_{(\theta_f, x_f, \theta_s)_{ss}} \right) & \dfrac{1}{\varepsilon} \left. \dfrac{\partial \mathbb{R}}{\partial \theta_s} \right|_{(\theta_f, x_f, \theta_s)_{ss}} \\ \dfrac{\mathrm{St}_h}{(\mathrm{Le} - \varepsilon)} & \dfrac{\beta}{(\mathrm{Le} - \varepsilon)} \left. \dfrac{\partial \mathbb{R}}{\partial x_f} \right|_{(\theta_f, x_f, \theta_s)_{ss}} & \dfrac{1}{(\mathrm{Le} - \varepsilon)} \left(-\mathrm{St}_h + \beta \left. \dfrac{\partial \mathbb{R}}{\partial \theta_s} \right|_{(\theta_f, x_f, \theta_s)_{ss}} \right) \end{bmatrix} \tag{45}$$

and

$$\mathbb{P}_2 = \begin{bmatrix} \frac{1}{\varepsilon}\frac{1}{\mathrm{Pe}^h_{f,\perp}} & 0 & 0 \\ 0 & \frac{1}{\varepsilon}\frac{1}{\mathrm{Pe}^m_{f,\perp}} & 0 \\ 0 & 0 & \frac{1}{(\mathrm{Le}-\varepsilon)}\frac{1}{\mathrm{Pe}^h_{s,\perp}} \end{bmatrix} \tag{46}$$

The neutral stability curve is obtained by a simultaneous solution of the uniform steady-state solutions of Eqs. 26–29 and

$$\det(\mathbb{L}^{\mathbb{SR}}_{\mathbb{TP}}) = 0 \tag{47}$$

Unfortunately, we were unable to derive in this case a bound on

$$\mathcal{M}_{\mathbb{TP}} = \frac{\mathrm{Pe}^m_{f,\perp}}{\mathrm{Pe}^h_{f,\perp}} = \frac{\lambda_{f,\perp}}{D_{f,\perp}(\rho C_p)_f} \tag{48}$$

above which a stable uniform state cannot bifurcate to a nonuniform state. Extensive calculations indicated that for the kinetic model used here a uniform steady state may bifurcate only to a stationary nonuniform state. However, we are unable to prove this.

Before proceeding to the regular reactor case, we shall present some numerical results describing the impact of $\mathcal{M}_{\mathbb{TP}}$ on the evolution of the nonuniform states for the two-phase $\mathbb{SR}$. In all the numerical simulations, unless otherwise stated, we used the following set of parameters

$$\varepsilon = 0.36 \qquad \mathrm{Le} = 1416$$

$$\beta = 0.4 \qquad \gamma = 15$$

$$\mathrm{St}_h = 300\frac{L}{d_p} \qquad \mathrm{St}_m = 200\frac{L}{d_p}$$

$$\mathrm{Pe}^h_{f,a} = \frac{L}{d_p} \qquad \mathrm{Pe}^m_{f,a} = 5.0\frac{L}{d_p}$$

$$\mathrm{Pe}^h_{s,a} = 0.25\frac{L}{d_p} \qquad \mathrm{Pe}^h_{f,\perp} = 2.0\frac{(R/d_p)^2}{L/d_p}$$

$$\mathrm{Pe}^h_{s,\perp} = 1.0\frac{(R/d_p)^2}{L/d_p} \tag{49}$$

We used $L = d_p$ in all the shallow reactor simulations and $L = 30d_p$ in all the regular reactor simulations. Figure 2 shows the neutral stability curve of the bifurcation to the first mode ($\mu_{mn} = 1.8412$) for the shallow reactor. Figure 2a shows that for $\mathcal{M}_{\mathbb{TP}} \geq 1$ the stability curve is bounded between the Da values corresponding to the ignition (Da_i) and extinction (Da_e). However, this graph does not show from which branch of uniform states the bifurcation occurs. Thus, from now on we report the stability curves in the plane of R/d_p vs. $\theta_{f,exit}$, the effluent temperature, because these plots show from which branch of uniform solutions the bifurcation occurs. Figure 2b shows that for all $\mathcal{M}_{\mathbb{TP}} \geq 1$, the bifurcation occurs from the branch of unstable uniform states because the effluent temperature is bounded between the ignition and extinction temperatures (θ_i and θ_e). However, for $\mathcal{M}_{\mathbb{TP}} = 0.165$ and $R/d_p > 7.5$ one bifurcation to nonuniform temperature state occurs from a stable, uniform high-temperature state ($\theta > \theta_e$), and a second one from an unstable, uniform temperature state ($\theta_e < \theta < \theta_i$). For $\mathcal{M}_{\mathbb{TP}} = 0.075$ and $R/d_p > 6.5$ one bifurcation is from a stable, uniform high-temperature state and the second from a stable, uniform low-temperature state.

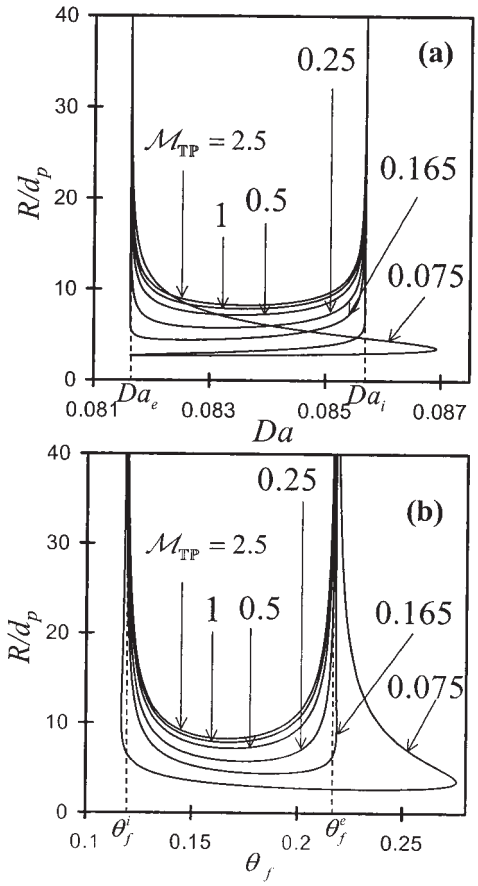

Figure 2. Neutral stability curves corresponding to the first transversal mode ($\mu_{mn} = 1.8412$) for a two-phase model of a shallow packed-bed reactor ($L = d_p$) for various $\mathcal{M}_{\mathbb{TP}}$ in (a) the R/d_p vs. Da and (b) R/d_p vs. $\theta_{f,\mathrm{exit}}$ plane.

Figure 3 is a bifurcation diagram of the uniform and nonuniform states of this reactor. The nonuniform states were obtained by perturbing the uniform ones close to the bifurcation points by the first mode and numerical continuation to compute the branch. The transition from uniform to nonuniform states occurred at a pitchfork bifurcation, at which a pair of nonuniform branches emerged. The nonuniform states bifurcating from a uniform unstable branch are unstable. In all the cases we studied, the pitchfork bifurcation from the branch of uniform stable states is subcritical, that is, the bifurcating nonuniform states are unstable. (In all the bifurcation diagrams shown here, except for Figure 10, dashed lines represent unstable transversal nonuniform states and solid segments on these branches represent stable transversal nonuniform states.) In the case shown in Figure 3 for $\mathcal{M}_{\mathbb{TP}} = 1.5$, all the states on the two nonuniform branches are unstable. In contrast, some of

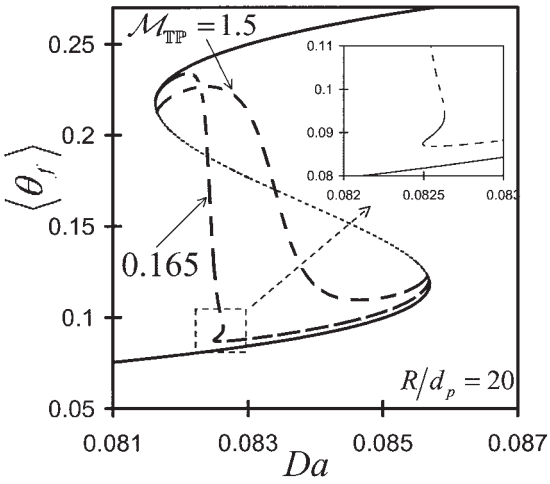

Figure 3. Dependency of the uniform and nonuniform states corresponding to the first mode on Da for a two-phase model of a shallow packed-bed reactor ($L = d_p$) for $\mathcal{M}_{TP} = 0.165$ and $\mathcal{M}_{TP} = 1.5$.

Dotted line denotes unstable uniform state; dashed line denotes unstable nonuniform state; solid line denotes stable states.

the nonuniform states for $\mathcal{M}_{TP} = 0.165$ are stable. The nonuniform states are rather similar in shape to the first mode, that is, half of the cross section is hot and half is cold. The neutral stability curve in Figure 2 indicates that for $\mathcal{M}_{TP} = 0.075$ and $R/d_p > 6.5$ the branch of the nonuniform state emanates from a stable, uniform ignited state and terminates at a stable, uniform extinguished state. In the special case of mode 1, the two states (on either branches of the nonuniform states) are mirror images of each other and have the same effluent temperature. Thus, the two states are represented by a single branch in Figure 3.

Figure 4 shows the neutral stability corresponding to the third mode ($\mu_{mn} = 3.8317$), which has no azimuthal dependency and has the shape of a target. Again, bifurcation from stable uniform states do not occur for values of $\mathcal{M}_{TP} \geq 1$. However, bifurcations from stable uniform states occur for sufficiently small values of $\mathcal{M}_{TP}$.

Figure 5 is a bifurcation diagram of the uniform steady states and the stationary nonuniform ones corresponding to the third mode. The states corresponding to $\mathcal{M}_{TP} = 1.5$ emanate from unstable, uniform states and all the states on this branch are unstable. For $\mathcal{M}_{TP} = 0.165$ the branch of nonuniform state bifurcates (subcritically) from a stable, uniform ignited state and terminates at an unstable, uniform state. Some of the nonuniform states on this branch are stable (solid line in Figure 5), whereas the others are unstable. The nonuniform states were rather similar in shape to the third mode, that is, had the shape of a target. Two branches of nonuniform states exist in this case. This occurs because the pitchfork bifurcation leads to formation of two nonuniform states that have different effluent temperatures.

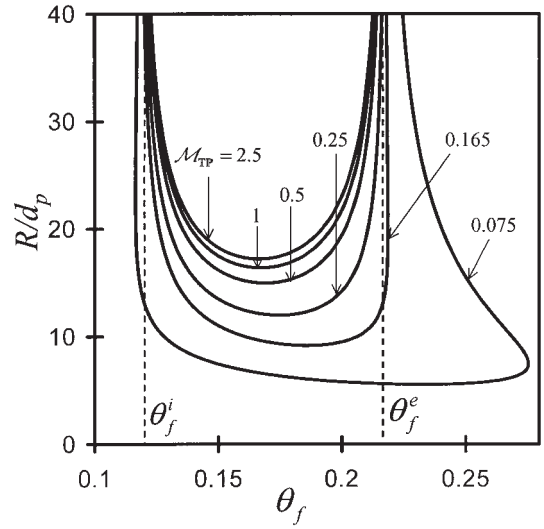

Figure 4. Neutral stability curves corresponding to the third transversal mode ($\mu_{mn} = 3.8317$) for a two-phase model of a shallow packed-bed reactor ($L = d_p$) for various $\mathcal{M}_{TP}$.

Stationary nonuniform temperature in packed-bed reactors

We consider here the formation of nonuniform transversal temperature patterns in an adiabatic packed-bed reactor using a two-phase model. At the neutral stability curve a transition from a uniform to a nonuniform state occurs following a nonuniform perturbation. It is obtained by solving simultaneously the transversally uniform steady-state form of equations (Eqs. 11–17) and the eigenvalue problem

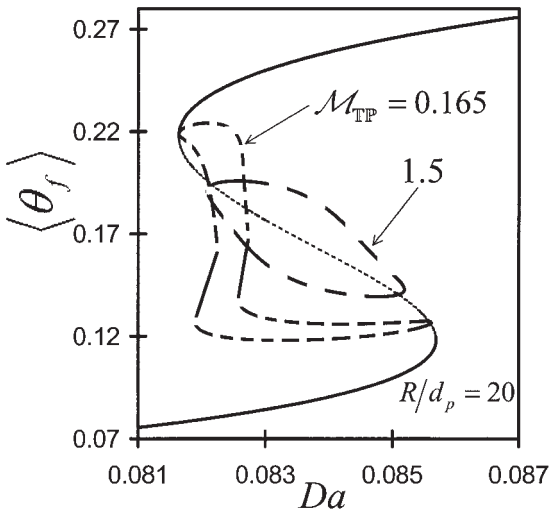

Figure 5. Dependency of the uniform and nonuniform states corresponding to the third mode on Da for a two-phase model of a shallow packed-bed reactor ($L = d_p$) for $\mathcal{M}_{TP} = 1.5$ and $\mathcal{M}_{TP} = 0.165$.

Dotted line denotes unstable uniform state; dashed line denotes unstable nonuniform state; solid line denotes stable states.

$$\frac{1}{\varepsilon}\left(\frac{1}{\mathrm{Pe}^h_{f,a}}\frac{\partial^2\omega_1}{\partial\eta^2}-\frac{\partial\omega_1}{\partial\eta}-\frac{\mu^2_{mn}\omega_1}{\mathrm{Pe}^h_{f,\perp}}+\mathrm{St}_h(\omega_3-\omega_1)\right)=\sigma\omega_1 \quad (50)$$

$$\frac{1}{\varepsilon}\left(\frac{1}{\mathrm{Pe}^m_{f,a}}\frac{\partial^2\omega_2}{\partial\eta^2}-\frac{\partial\omega_2}{\partial\eta}-\frac{\mu^2_{mn}\omega_2}{\mathrm{Pe}^m_{f,\perp}}+\left.\frac{\partial\mathbb{R}}{\partial x_f}\right|_{(\theta_f,x_f,\theta_s)_{ss}}\omega_2+\left.\frac{\partial\mathbb{R}}{\partial\theta_s}\right|_{(\theta_f,x_f,\theta_s)_{ss}}\omega_3\right)=\sigma\omega_2 \quad (51)$$

$$\frac{1}{\mathrm{Le}-\varepsilon}\left(\frac{1}{\mathrm{Pe}^h_{s,a}}\frac{\partial^2\omega_3}{\partial\eta^2}-\frac{\mu^2_{mn}\omega_3}{\mathrm{Pe}^h_{s,\perp}}-\mathrm{St}_h(\omega_3-\omega_1)+\beta\left.\frac{\partial\mathbb{R}}{\partial x_f}\right|_{(\theta_f,x_f,\theta_s)_{ss}}\omega_2+\beta\left.\frac{\partial\mathbb{R}}{\partial\theta_s}\right|_{(\theta_f,x_f,\theta_s)_{ss}}\omega_3\right)=\sigma\omega_3 \quad (52)$$

subject to the boundary conditions

$$\frac{1}{\mathrm{Pe}^h_{f,a}}\frac{\partial\omega_1}{\partial\eta}=\omega_1 \quad \frac{1}{\mathrm{Pe}^m_{f,a}}\frac{\partial\omega_2}{\partial\eta}=\omega_2 \quad \frac{\partial\omega_3}{\partial\eta}=0 \quad \eta=0 \quad (53)$$

$$\frac{\partial\omega_1}{\partial\eta}=\frac{\partial\omega_2}{\partial\eta}=\frac{\partial\omega_3}{\partial\eta}=0 \quad \eta=1 \quad (54)$$

$$\frac{\partial\omega_1}{\partial\xi}=\frac{\partial\omega_2}{\partial\xi}=\frac{\partial\omega_3}{\partial\xi}=0 \quad \xi=1 \quad (55)$$

Linear stability predicts the nature of the bifurcating nonuniform solutions. When a single negative eigenvalue σ becomes positive upon crossing the neutral stability curve, a stationary nonuniform state evolves, whereas if a pair of complex eigenvalues crosses the imaginary axis an oscillatory nonuniform state evolves. Extensive numerical simulations suggest that this three-variable model leads only to bifurcations to a stationary nonuniform state, although we could not prove this. Similarly, we were unable to derive a criterion predicting the impact of the ratio between the effective transversal dispersion of heat and mass on the stability of the uniform steady state from which the nonuniform states can bifurcate.

Figure 6 shows the neutral stability curve of the bifurcation to the first mode ($\mu_{mn} = 1.8412$). Figure 6a shows that for all $\mathcal{M}_{\mathbb{TP}} \geq 1$ the stability curve is bounded between the Da values corresponding to the ignition (Da_i) and extinction (Da_e). Figure 6b shows that for all $\mathcal{M}_{\mathbb{TP}} \geq 1$ the nonuniform states bifurcate from the branch of unstable uniform states because their effluent temperature is between the ignition and extinction temperatures (θ_i and θ_e). This indicates that, as predicted by the shallow reactor model, no bifurcation from a stable uniform steady-state solution can occur under the practical case of $\mathcal{M}_{\mathbb{PH}} \geq 1$. However, for $\mathcal{M}_{\mathbb{TP}}$ values of 0.1 and 0.075 bifurcations to nonuniform temperature state occur from the stable, uniform high-temperature states ($\theta > \theta_e$). The qualitative behavior of this model is similar to that of the shallow reactor shown in Figure 2. However, a nonuniform state bifurcated from stable uniform states for $\mathcal{M}_{\mathbb{TP}} = 0.165$ for the shallow reactor. No such bifurcation occurred in the regular packed-bed reactor model. Numerical simulations indicated that when the neutral

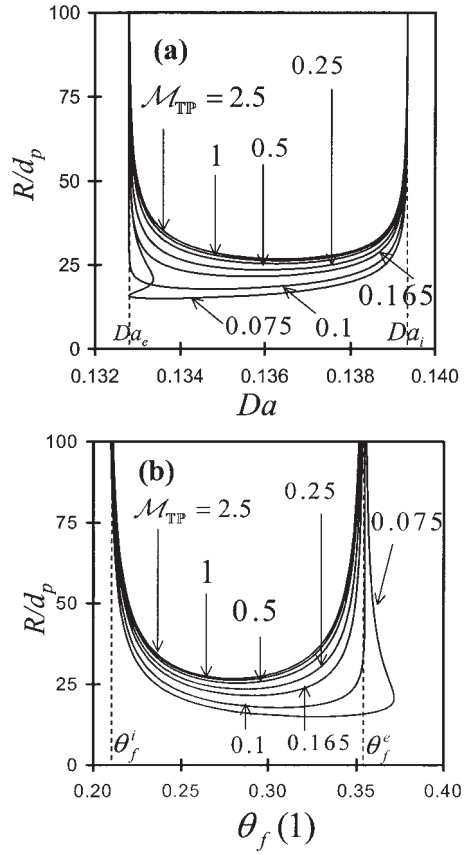

Figure 6. Neutral stability curves corresponding to the first transversal mode (μ_{mn} = 1.8412) for a two-phase model of a packed-bed reactor (L = 30d_p) for various $\mathcal{M}_{\mathbb{TP}}$ in (a) the R/d_p vs. Da and (b) R/d_p vs. $\theta_{f,\mathrm{exit}}$ plane.

stability curve has a fold in the (R/d_p vs. Da) plane, such as for $\mathcal{M}_{\mathbb{TP}} = 0.075$ in Figure 6a, then a bifurcation can occur from a stable uniform state.

The neutral stability curves for the higher modes have a shape similar to that for mode 1. For example, Figure 7 shows the neutral stability for nonuniform states corresponding to the third mode ($\mu_{mn} = 3.8317$) in Figure 1. Again, bifurcation from stable uniform states do not occur for values of $\mathcal{M}_{\mathbb{TP}} \geq 1$. However, bifurcations from stable uniform state occur for sufficiently small values of $\mathcal{M}_{\mathbb{TP}}$. Comparison of Figures 6b and 7 shows that the neutral stability curve for the higher mode are shifted to higher values of R/d_p. The fact that the neutral stability curves for higher modes are shifted to higher values of R/d_p implies that the larger the reactor diameter, the larger the number of possible stationary nonuniform states.

The bifurcation diagram of the uniform steady state and of the nonuniform ones corresponding to the third mode are shown in Figure 8. The states corresponding to $\mathcal{M}_{\mathbb{TP}} = 1.5$ emanate from unstable, uniform states and all the states on this branch are unstable. This occurs for all the states satisfying the realistic condition that $\mathcal{M}_{\mathbb{PH}} \geq 1$. For $\mathcal{M}_{\mathbb{TP}} = 0.075$ the branch of nonuniform state bifurcates (subcritically) from a stable, uniform ignited state and terminates at an unstable, uniform state. Some of the nonuniform states on that branch are stable

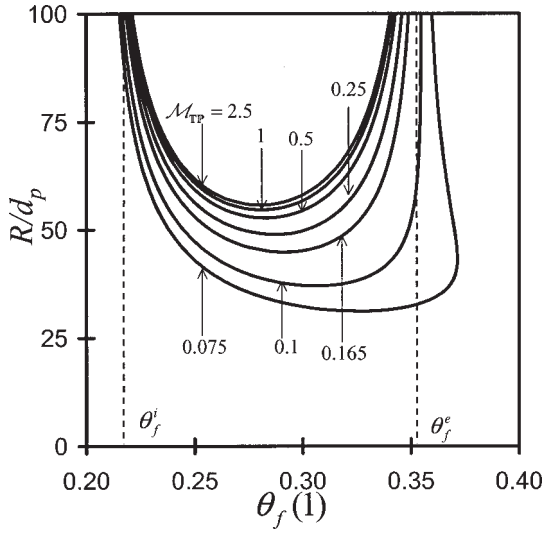

Figure 7. Neutral stability curves corresponding to the third transversal mode (μ_{mn} = 3.8317) for a two-phase model of a packed-bed reactor (L = 30d_p) for various $\mathcal{M}_{\mathbb{TP}}$.

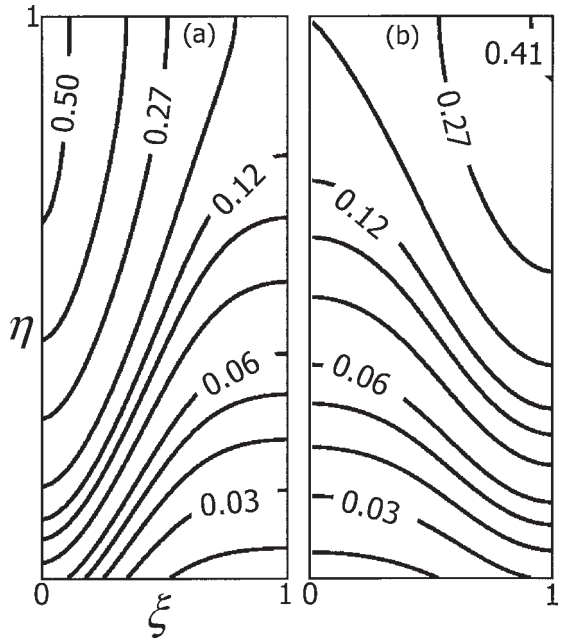

Figure 9. Reactor temperature of stable nonuniform states in a packed-bed reactor predicted by a two-phase model and corresponding to the third mode for Da = 134 and $\mathcal{M}_{\mathbb{PH}}$ = 0.075 when (a) $\langle\theta_{f,\text{exit}}\rangle$ = 0.237 and (b) $\langle\theta_{f,\text{exit}}\rangle$ = 0.325.

(solid line in Figure 8), whereas the others are unstable. The nonuniform states are rather similar in shape to the third mode. Two branches of nonuniform states exist in this case. This occurs because the pitchfork bifurcation leads to formation of two nonuniform states with different effluent temperatures.

The solutions corresponding to mode 3 have no azimuthal dependency and have the shape of a target at any cross section of the reactor. Figure 9 describes the temperature profiles within such a reactor of such a stable nonuniform state. It was computed for $\mathcal{M}_{\mathbb{TP}}$ = 0.075. Thus, it corresponds to the condition that the effective heat diffusivity is smaller than that of the limiting reactant.

The branches of the nonuniform states corresponding to the second mode (μ_{mn} = 3.0542) are shown in Figure 10 for $\mathcal{M}_{\mathbb{TP}}$ = 1.5, that is, for a realistic situation, in which the heat dispersion exceeds that of the limiting reactants. In this case the two branches of the nonuniform states emanate from an unsta-

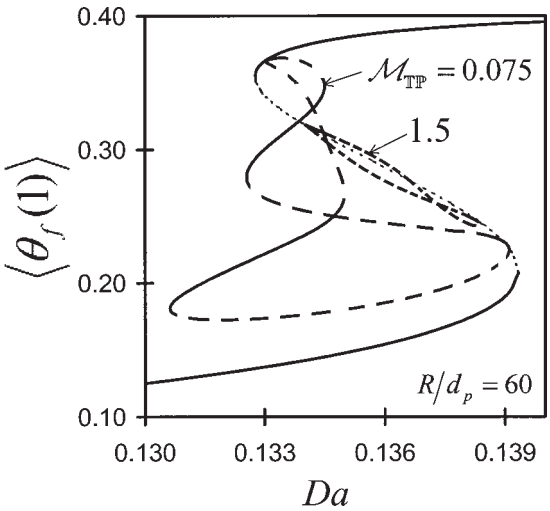

Figure 8. Dependency of the uniform and nonuniform states corresponding to the third mode on Da for a two-phase model of a packed-bed reactor (L = 30d_p) for $\mathcal{M}_{\mathbb{TP}}$ = 1.5 and $\mathcal{M}_{\mathbb{TP}}$ = 0.075.

Dotted line denotes unstable uniform state; dashed line denotes unstable nonuniform state; solid line denotes stable states.

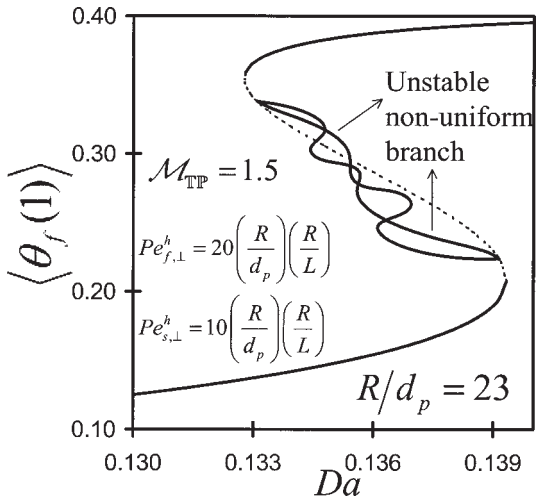

Figure 10. Dependency of the uniform and nonuniform states corresponding to the second mode on Da for a two-phase model of a packed-bed reactor (L = 30d_p) for $\mathcal{M}_{\mathbb{TP}}$ = 1.5.

Dotted line denotes unstable uniform state; dashed line denotes unstable nonuniform state; solid line denotes stable states.

ble uniform steady state, located on the intermediate branch of solutions. Detailed linear stability calculations showed that all the states on the two branches were unstable and there was no change in stability at the limit points on the branches of these states.

Conclusions and Remarks

A pseudo-homogeneous model predicts that a stable, stationary nonuniform temperature pattern cannot form in any cross section of an adiabatic packed-bed reactor used to carry out a single reaction, having a conventional rate expression that accounts only for reactant surface adsorption, desorption, and temperature. This is explained by the fact that the transversal heat dispersion in the reactor is larger than that of the limiting reactant. This conclusion is true for all the possible modes. This conclusion was proved for a shallow packed-bed reactor described by a pseudo-homogeneous model. Extensive numerical simulations showed that both a regular and shallow packed-bed reactor described by a two-phase model exhibited the same qualitative behavioral features. A stable, stationary pattern may form in the cross section of the reactor only under the assumption that the transversal species dispersion exceeds that of the temperature. As indicated by Schmitz and Tsotsis[14] and Yakhnin and Menzinger,[17] this condition is not satisfied in packed-bed reactors and is the same as that generating a Turing pattern in reaction–diffusion systems.

This study shows that the analysis of pattern formation in a shallow packed-bed reactor provides useful insight and guidance about pattern evolution and stability in packed-bed reactors. Moreover, it drastically decreases the numerical effort needed to conduct such studies. This finding should be used in future studies of pattern formation involving different classes of reactions.

Our study is the first to present the branches of stationary transversal pattern states in a 3D packed-bed reactor. We found that all the stationary patterned states on the branch were unstable, when the branch bifurcated from two states that were unstable to uniform disturbances. Stable stationary states were obtained only when the branch bifurcated from a uniform state stable to uniform disturbances. Only some of the states on the branch of nonuniform states were stable.

The analysis of the pattern formation in an adiabatic packed-bed reactor exploits the fact that the concentration and temperature satisfy the same (no-flux) boundary condition at the reactor walls. Consequently, the radial perturbations of all the variables can be expressed by the same Bessel functions. A much more intricate analysis is required when heat transfer occurs at the reactor walls. In this case different Bessel functions describe the concentration and temperature disturbances and the concentration and temperature patterns are no longer similar. It is important to conduct future analysis of this case to gain insight into the impact of the heat losses on the pattern evolution and stability.

This study, however, does not provide an answer to the important question: Which reaction mechanism and operating condition can lead to transversal pattern formation in adiabatic packed-bed reactors? Several industrial reports and laboratory experiments mentioned in the introduction reported formation of hot zones in packed-bed reactors. This study suggests that a bifurcation to a stable nonuniform state may occur only if the reaction rate depends—in addition to the temperature and surface adsorption and desorption of reactants—on other rate processes, such as a periodic variation of the surface catalytic activity[33]or impact of subsurface adsorption–desorption of reactants.[34,35] The pattern formation for these more complex kinetic mechanisms will be addressed in a future publication. Our analysis is of a bed that is uniformly packed with no internal flow obstructions. Clearly, internal obstruction of the flow[36] or nonuniform packing of the bed[8] may also generate hot zones.

Acknowledgments

We gratefully acknowledge support of this research by grants from the National Science Foundation, the Welch Foundation and the San Diego Supercomputing Center. We thank Dr. Andrew Salinger for helpful discussions and advice.

Notation

a_v = specific surface area, m^2/m^3
C = concentration, mol/m^3
C_p = specific heat capacity, J kg^{-1} k^{-1}
d_p = diameter of particle, m
D = species diffusion coefficient, m^2/s
Da = Damköhler number
E = activation energy, J/mol
h = interfacial heat transfer coefficient, W K^{-1} m^{-2}
J = Bessel function of first kind
k = interfacial mass transfer coefficient, m/s
k_∞ = intrinsic reaction rate constant, 1/s
L = reactor length, m
$\mathbb{L}$ = first Fréchet derivative
Le = Lewis number, defined by Eq. 10
$\mathrm{Le}_{\mathbb{PH}}$ = Lewis number, defined by Eq. 24
$\mathcal{M}$ = ratio of transversal heat to mass dispersions
N = radial grid points
$\mathbb{P}$ = transversal perturbation matrix
Pe = Peclet number, defined by Eq. 10
$\mathrm{Pe}_{\mathbb{PH}}$ = Peclet number, defined by Eq. 24
r = radial coordinate, m
R = reactor radius, m
$\bar{r}$ = reaction rate, mol m^{-3} s^{-1}
$\mathbb{R}$ = dimensionless reaction rate
$\bar{R}$ = universal gas constant, J mol^{-1} K^{-1}
St_m = Stanton number for mass, defined by Eq. 10
St_h = Stanton number for heat, defined by Eq. 10
t = time, s
T = temperature, K
v = linear velocity, m/s
x = conversion, defined by Eq. 10
z = axial coordinate, m

Greek letters

β = adiabatic temperature rise, defined by Eq. 10
γ = dimensionless activation energy, defined by Eq. 10
ε = bed voidage
η = dimensionless axial coordinate
θ = dimensionless temperature, defined by Eq. 10
λ = thermal conductivity, *W/(m.K)*
μ = transversal eigenmode number
ξ = dimensionless radial coordinate
σ = eigenvalue
τ = dimensionless time, defined by Eq. 10
ϕ = azimuthal coordinate
ω_i = *i*th component of nonuniform perturbation
$-\Delta H$ = heat of the reaction, J/mol

Other

$\langle \cdot \rangle$ = averaged quantity

Subscripts

a = axial
f = fluid phase
in = inlet
m = azimuthal mode number
n = radial mode number
$\mathbb{PH}$ = pseudo-homogeneous
s = solid phase
ss = transversally uniform steady state
$\mathbb{TP}$ = two-phase
$\perp$ = transversal

Superscripts

e = extinction
h = mass
i = ignition
m = mass
$\mathbb{SR}$ = shallow reactor

Literature Cited

1. Puszynski J, Hlavacek V. Experimental study of ignition and extinction waves and oscillatory behavior of a tubular non-adiabatic fixed-bed reactor for the oxidation of CO. *Chem Eng Sci.* 1984;39:681-691.
2. Wicke E, Onken HU. Periodicity and chaos in a catalytic packed bed reactor for CO oxidation. *Chem Eng Sci.* 1988;43:2289-2294.
3. Wicke E, Onken HU. Bifurcation, periodicity and chaos by thermal effects in heterogeneous catalysis. In: Markus M, Muller SC, Nicolis G, eds. *From Chemical to Biological Organization.* Berlin/New York, NY: Springer-Verlag; 1988:68-81.
4. Rovinski AB, Menzinger M. Self-organization induced by the differential flow of activator and inhibitor. *Phys Rev Lett.* 1993;70:778-781.
5. Sheintuch M, Shvartsman S. Spatiotemporal patterns in catalytic reactors. *AIChE J.* 1996;42:1041-1068.
6. Sheintuch M. Pattern selection in a general model of convection, diffusion, and catalytic reaction. *Physica D.* 1997;102:125-146.
7. Sheintuch M, Nekhamkina O. Pattern formation in models of fixed-bed reactors. *Catal Today.* 2001;70:369-382.
8. Matros YS. *Unsteady Processes in Catalytic Reactors.* Amsterdam: Elsevier; 1985.
9. Barkelew CH, Gambhir BS. Stability of trickle-bed reactors. *ACS Symp Ser.* 1984;237:61-81.
10. Viljoen HJ, Gatica JE, Hlavacek V. Bifurcation analysis of chemically driven convection. *Chem Eng Sci.* 1990;45:503-517.
11. Stroh F, Balakotaiah V. Modeling of reaction induced flow maldistributions in packed beds. *AIChE J.* 1991;37:1035-1052.
12. Nguyen D, Balakotaiah V. Flow maldistributions and hot spots in down-flow packed bed reactors. *Chem Eng Sci.* 1994;49:5489-5505.
13. Nguyen D, Balakotaiah V. Reaction-driven instabilities in down-flow packed beds. *Proc R Soc Lond A Phys Sci* 1995;450:1-21.
14. Subramanian S, Balakotaiah V. Analysis and classification of reaction driven stationary convective patterns in a porous medium. *Phys Fluids.* 1997;9:1674-1695.
15. Schmitz RA, Tsotsis TT. Spatially patterned states in systems of interacting catalyst particles. *Chem Eng Sci.* 1983;38:1431-1437.
16. Balakotaiah V, Christaforatou EL, West DH. Transverse concentration and temperature non-uniformities in adiabatic packed bed catalytic reactors. *Chem Eng Sci.* 1999;54:1725-1734.
17. Yakhin V, Menzinger M. On transverse patterns in catalytic packed bed reactors. *Chem Eng Sci.* 2001;56:2233-2236.
18. Turing A. The chemical basis for morphogenesis. *Philos Trans R Soc London B Biol Sci* 1952;237:37-72.
19. Segal LA, Jackson JL. Dissipative structure: An explanation and an ecological example. *J Theor Biol.* 1972;37:545-559.
20. Vortmeyer D, Schaeffer RJ. Equivalence of one- and two-phase models for heat transfer processes in packed beds: One dimensional theory. *Chem Eng Sci.* 1974;29:485-491.
21. Balakotaiah V, Dommeti SMS. Effective models for packed bed catalytic reactors. *Chem Eng Sci.* 1999;54:1621-1638.
22. van der Vorst HA. BI-CGSTAB: A fast and smoothly converging variant of BI-CG for the solution of nonsymmetric linear systems. *SIAM J Sci Stat Comput.* 1992;13:631-644.
23. Nowak U, Weimann L. A family of Newton codes for systems of highly nonlinear equations—Algorithm, implementation, application. Technical Report TR90-10. Berlin-Dahlem, Germany: Konrad-Zuse-Zentrum für Informationstechnik; 1990.
24. Keller HB. Numerical solutions of bifurcation and nonlinear eigenvalue problems. In: Rabinowitz PH, ed. *Applications to Bifurcation Theory: Proceedings of an Advanced Seminar.* New York, NY: Academic Press; 1977:159-385.
25. Salinger AG, Burroughs EA, Pawlowski RP, Phipps ET, Romero LA. Bifurcation tracking algorithms and software for large scale applications. *Int. J. Bif. and Chaos*. 2005;15:1015-1032.
26. Burroughs EA, Ramero LA, Lehoucq RB, Salinger AG. Large scale eigenvalue calculations for computing the stability of buoyancy driven flows. Sandia Technical Report 2001-0113. Albequerque, NM: Sandia National Laboratories (SAND); 2003.
27. Deuflhard P, Hairer E, Zugck J. One-step extrapolation methods for differential-algebraic systems. *J Numer Math.* 1987;51:501-516.
28. Ehrig R, Nowak U, Oeverdieck L, Deuflhard P. Advanced extrapolations methods for large scale differential algebraic problems. In: Bungartz H-J, Durst F, Zenger Chr, eds. *High Performance Scientific and Engineering Computing.* (Lecture Notes in Computational Science and Engineering). Vol. 8. Munich, Germany: Springer-Verlag; 1999:233-244.
29. Balakotaiah V, Gupta N, West DH. Transport limited pattern formation in catalytic monoliths. *Chem Eng Sci.* 2002;57:435-448.
30. Golubitsky M, Schaeffer DG. *Singularities and Groups in Bifurcation Theory*. Vol. I. New York, NY: Springer-Verlag; 1984.
31. Viswanathan GA. *Transversal Temperature Patterns in Packed Bed Reactors.* PhD Dissertation. Houston, TX: University of Houston; 2004.
32. Middya U, Luss D. Impact of global interaction on pattern formation on a disk. *J Chem Phys.* 1995;102:5029-5036.
33. Krischer K, Eiswirth M, Ertl G. Oscillatory CO oxidation on Pt(110): Modeling of temporal self-organization. *J Chem Phys.* 1992;96:9161-9172.
34. Ivanov EA, Chumakov GA, Slinko MG, Bruns DD, Luss D. Isothermal sustained oscillations due to the influence of adsorbed species on the catalytic reaction rate. *Chem Eng Sci.* 1980;35:795-803.
35. Sales BC, Turner JE, Maple MB. Oscillatory oxidation of CO over a Pt catalyst. *Surf Sci.* 1981;103:54-74.
36. Jaffe SB. Hot spot simulation in commercial hydrogenation processes. *Ind Eng Chem Process Des Dev.* 1976;15:410-416.

Manuscript received Dec. 23, 2004, and revision received Mar. 7, 2005.